DOI: 10.63527/1607-8829-2025-1-81-100

R.R. Kobylianskyi[1,2] (https://orcid.org/0000-0002-4664-3162),
O.I. Ivaschuk[3] (https://orcid.org/0000-0003-1747-2648),
V.Yu. Bodiaka[3] (https://orcid.org/0000-0003-1422-6652),
R.V. Fedoriv[1] (https://orcid.org/0009-0005-4487-9365)

[1]Yury Fedkovych Chernivtsi National University,
2 Kotsiubynsky str., Chernivtsi, 58012, Ukrainea;
[2]Institute of Thermoelectricity of the NAS and MES
of Ukraine, 1 Nauky str., Chernivtsi, 58029, Ukraine;
[3]Bukovinian State Medical University,
2 Theater Square, Chernivtsi, 58002, Ukraine

Corresponding author: R.R. Kobylianskyi, e-mail: *romakobylianskyi@ukr.net*

Computer Optimization of the Working Tool for a Thermoelectric Cryodestruction Device

The paper presents the results of computer simulation of the temperature impact on biological tissue with an oncological neoplasm in the cooling mode. A physical, mathematical and computer model of biological tissue with an oncological neoplasm was constructed taking into account thermophysical processes, blood circulation, heat exchange, metabolic processes and phase transition. Computer optimization of the working tool and calculation of the heat removal system of thermoelectric modules for a thermoelectric cryodestruction device were carried out. Temperature distributions in biological tissue and the cooling working tool were determined. The results obtained make it possible to determine the freezing depth of biological tissue, in particular of oncological neoplasms, at a given temperature impact. A method of computer calculation of the temperature impact on biological tissues has been developed, which allows obtaining temperature distributions inside biological tissue and predicting the freezing depth during cryodestruction.

Key words: thermoelectricity, thermoelectric device, working tool, computer optimization, computer simulation, cryodestruction, temperature impact, cooling mode, temperature distribution, biological tissue, oncological neoplasm.

Introduction

Modern thermoelectricity is a rapidly developing area of science and technology and is finding ever wider application. Thermoelectric energy conversion is based on thermoelectric

Citation: R.R. Kobylianskyi, O.I. Ivaschuk, V.Yu. Bodiaka, R.V. Fedoriv (2025). Computer Optimization of the Working Tool for a Thermoelectric Cryodestruction Device. *Journal of Thermoelectricity*, (1), 81–100. https://doi.org/10.63527/1607-8829-2025-1-81-100

phenomena [1 – 3], the application of which allows the use of thermoelectric converters in various industries, in particular in medicine. Improving the quality of thermoelectric materials and modules [4 – 8] that form the basis of thermoelectric equipment for medical purposes is of great importance.

According to statistics [9], about 310 million surgical operations are performed annually in the world. Each of these operations is risky, but its successful implementation gives a person a chance to return to a normal lifestyle. According to the World Health Organization (WHO), about 15 % of all surgical operations are accompanied by serious complications, and the mortality rate during operations is 1 – 4 %. This means that the annual global mortality after surgical operations is about 8 million patients and places major surgical interventions among the leading causes of death, along with cardiovascular diseases, stroke, oncology and injuries [10].

It is known that treatment with antibiotics and other drugs is not always effective, since the human body has the property of getting used to some drugs. It has been established [11 – 19] that when low temperatures are applied to the affected area of biological tissue, all pathogenic microorganisms die, and that cold activates the immune system of the human body, mobilizes the endocrine and neurohumoral systems, provides resistance to stress and overload, improves a person's well-being and working capacity. The use of cryodestruction allows improving the results of treatment of many diseases in such areas of medicine as neurosurgery, oncology, gynecology, urology, proctology, otolaryngology, ophthalmology, traumatology, reflexology, dermatology, cosmetology, etc. [20 – 31].

As is known, the cell structures of different biological objects differ from each other in water content, the ratio of biological elements and electrolytic composition. These physical and chemical indicators mainly determine different critical temperatures. As shown by a number of experimental studies on determining the vital activity of tumor cells, when exposed to $T_x = -15 \div -20$ °C, relapses occur in half of cases, at $T_x = -30$ °C – in 20 %, and at $T_x = 45 \div 50$ °C, a complete stop of tumor growth is observed [11-19]. The authors of [11] conducted studies on the dependence of the thermal conductivity of various tumors (hemangioma, melanoma, etc.) on temperature. It was found that in the temperature range from – 20 to – 18 °C, phase transitions completely stop and the values of thermal conductivity of biological tissue decrease. This is due to the appearance of microcracks in tissues during freezing, which in turn leads to an increase in thermal resistance and a decrease in thermal conductivity. In [11], the dependences of thermal conductivity of hemangioma and melanoma of different morphological structure and localization on temperature are given. As can be seen, with an equal amount of water (76 %), the values of thermal conductivity of different types of hemangioma are different. This suggests that thermal conductivity depends on the type of biological tissue, its localization and the amount of free water.

It was shown that the thermal conductivity curves during freezing and thawing do not coincide (hysteresis phenomenon), which is probably explained by the change of the "particle-ice" thermal contact to the ice-water" contact. The differences in the values of thermal conductivity during freezing and thawing in the temperature range from – 20 °C to 0° C are about 25 %. Therefore, it can be considered that the most effective in terms of destroying tumor tissue are

temperatures in the range from – 5 °C to – 50 °C [11 – 19], which corresponds to the temperature range in which thermoelectric devices are effective.

The use of cryodestruction for the treatment of oncological diseases allows avoiding the spread of metastases during surgical operations and reduces blood loss and provides an anesthetic effect. However, despite obvious successes, the process of introducing thermoelectric principles of obtaining cold into medicine is still too far from completion. The study of the use of low temperatures during surgical operations requires a comprehensive in-depth study of the features of the physicochemical processes in the field of cryotherapy in healthy and affected biological tissues, which is a complex task requiring the creation of accurate physical and mathematical models and the use of computer simulation.

The purpose of this work is computer optimization of the working tool for a thermoelectric cryodestruction device and creation of a computer simulation method that will allow predicting the results of local temperature effects on biological tissue during cryodestruction of oncological neoplasms.

1. Physical, mathematical and computer model of a thermoelectric cryodestruction device

Predicting the consequences of cryoimpact is a multifactorial problem, which, with the development of the cryosurgical treatment method, requires a simple and accessible method of prediction based on the relationship of variable parameters, such as temperature, geometry of the cryo tool, cooling rate and time of its exposure, and the volume and structure of biological tissues subject to cryodestruction.

To solve such problems, the method of analytical simulation of frozen tissue is usually used.

There are a sufficient number of models describing freezing processes around a cryo tool, differing in the degree of complexity [32 – 34]. Analytical modeling of the assessment of the sizes of freezing zones is important as a method of analyzing and optimizing the effectiveness of cryodestruction and as a basis for calculating the designs of cryo tools and deep cooling systems for cryosurgical equipment. The breadth of implementation of methods of mathematical prediction of the results of cryotherapy will depend primarily on the probability of describing the thermal processes occurring during freezing of biological tissues and the accompanying phase transitions.

In order to predict the results of local cryotherapy in advance, a physical (Fig. 1), mathematical and computer model (Fig. 2) of a device for cryodestruction of malignant oncological neoplasms was developed.

Structurally, the device consists of a working tool surrounded by insulation, two two-stage thermoelectric modules, on the hot side of which liquid heat exchangers are installed, a pump that pumps water through the channels, a fan and a liquid-air heat exchanger that cools the pumped liquid. Since cryodestruction requires achieving the lowest possible temperature values, two-stage thermoelectric modules ALTEC-011 are used, which are characterized by an increased temperature difference $\Delta T_{\max}$.

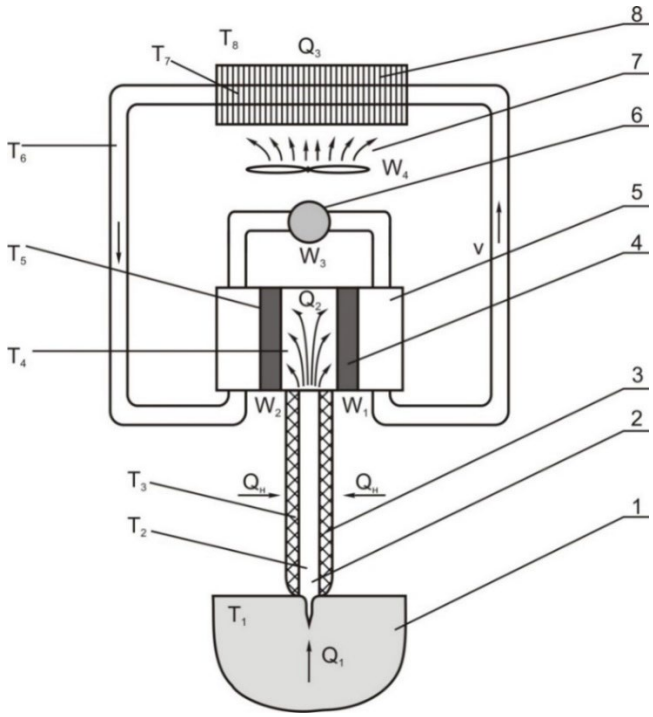

Fig. 1. Physical model of a thermoelectric device for the destruction of oncological neoplasms: 1 – tumor, 2 – working tool, 3 – insulation, 4 – two-stage thermoelectric module, 5 – liquid heat exchanger, 6 – pump, 7 – fan, 8 – liquid-air heat exchanger

Heat flow to thermoelectric modules:

$$Q_2 = Q_1 + Q_H\,, \tag{1}$$

where Q_1 is heat flow from the liver, Q_H is heat in-leak through the lateral surface of the working tool.

Heat flow after thermoelectric modules:

$$Q_3 = Q_2 + W\,, \tag{2}$$

where W is power of modules.

Heat flow transferred to the liquid from the hot side of the thermoelectric modules

$$Q_4 = \alpha_4 S_4 \left(T_5 - T_6\right). \tag{3}$$

Heat flow transferred to the liquid-air heat exchanger from the liquid:

$$Q_5 = \alpha_5 S_5 \left(T_6 - T_7\right). \tag{4}$$

Heat flow transferred from a liquid-air heat exchanger to the environment:

$$Q_6 = \alpha_6 S_6 \left(T_7 - T_8\right). \tag{5}$$

where α_4, α_5, α_6 are heat exchange coefficients, S_4, S_5, S_6 are heat exchange surface areas.

To find temperature distributions in the structural elements of the device for tumor cryodestruction and in the tumor itself, the Comsol Multiphysics application software package [35] was used, which allows simulation of thermophysical processes in biological tissues taking into account blood circulation, heat exchange, metabolic processes, and phase transition.

The heat transfer equation in biological tissue in this case will have the form [36]

$$\rho C_p \frac{\partial T}{\partial t} + \nabla\left(-\kappa \nabla T\right) = \rho_b C_b \omega_b \left(T_b - T\right) + Q_{met}, \quad (6)$$

where: ρ_b – blood density (kg/m^3), which is equal to the mass of blood divided by its volume; C_b – specific heat capacity (J/kg·K), which is equal to the amount of thermal energy required to create a unit temperature difference in a unit mass of blood; ω_b – blood flow rate (1/s), which in this case means (m^3/s)/m^3, and describes the volume of blood per second flowing through a unit volume of tissue; T_b – arterial blood temperature (K), equal to 310.15 K; Q_{met} – amount of metabolic heat (W/m^3).

The computer model represents a volume of biological tissue with isotropic thermal properties. Inside the biological tissue is placed a needle made of a material with high thermal conductivity, fixed on a rod made of the same material. The rod is surrounded by thermal insulation, which is in a state of heat exchange with the surrounding environment. The temperature at the end of the rod is given, and is equal to – 50 °C. The boundary condition is in the region far from the probe, where the temperature should be the same as the body temperature 37 °C. During the freezing process, biological tissue will undergo a phase change at the freezing point, with losses of latent heat of phase transition and the temperature in the biological tissue remaining unchanged. The phase transition in biological tissues occurs at temperatures from – 1 to – 8 °C. The properties of biological tissue in the frozen and thawed states are given in Table 1. In the temperature range of – 1 ÷ – 8 °C, when biological tissue is frozen, the latent heat of the phase transition is absorbed, which can be modeled by adding the corresponding value to the heat capacity [37 – 39]. The computer model of biological tissue with an oncological neoplasm and a working tool takes into account thermophysical processes, blood circulation, heat exchange, metabolic processes and phase transition.

Table 1

Properties of biological tissue in frozen and thawed states [40 – 48]

	Measurement units	Value
Heat capacity of frozen tissue	MJ/m^3 °C	1.8
Heat capacity of frozen tissue	MJ/m^3 °C	3.6
Heat capacity of blood	MJ/m^3 °C	3.6
Thermal conductivity of thawed tissue	W/m °C	0.5
Thermal conductivity of thawed tissue	W/m °C	2
Latent heat	MJ/m^3	250
Body temperature	°C	37
Lower phase transition temperature	°C	– 8
Upper phase transition temperature	°C	– 1
Blood perfusion in healthy tissue	ml/s/ml	0.0005
Blood perfusion in tumor	ml/s/ml	0.002
Metabolism in normal tissue	W/m^3	4200
Metabolism in tumor	W/m^3	42000

When biological tissue is frozen, the capillaries constrict until all the blood in the capillaries freezes, and the value of ω_b approaches zero. In addition, cells will not be able to generate metabolic heat when frozen, and Q_{met} will be zero at temperatures below zero.

2. Optimization of the working tool and calculation of the heat removal system of thermoelectric modules

2.1. Calculation of the cooling system of thermoelectric modules

An important task in the design of thermoelectric devices is the selection of the required type of heat exchanger. The main indicator that determines the area of expedient use of the cooling method is the density of heat flow passing through the surface of the heat exchanger.

The second indicator necessary for choosing a cooling method is the maximum permissible overheating of the elements ΔT_c.

The efficiency of a particular type of heat exchanger is determined by the heat transfer coefficient, which is given for different types of heat exchange and type of coolant:

1) free convection and evaporation 2 – 19 W/m^2 K
2) forced convection in gases 10 – 100 W/m^2 K
3) free convection in viscous liquids 200 – 300 W/m^2 K

Let us consider the calculation of "solid-liquid" heat exchanger.

The process of heat transfer during the movement of a coolant in a pipe (channel) depends on many factors. The laminar or turbulent flow regime is determined by the Reynolds number Re:

$$\mathrm{Re} = \frac{ud}{v}. \tag{7}$$

where u is the average (over the pipe cross section) fluid velocity, d is the internal diameter of the pipe.

When $Re < Re_{rh1} = 2300$ – the flow is laminar (Re_{rhl} – lower critical Reynolds number). When $Re < Re_{rh2} = 10000$, a developed turbulent flow is observed (Re_{rh2} – upper critical Reynolds number). Reynolds numbers lying in the interval $Re_{rh1} < Re < Re_{rh2}$, correspond to the transient flow mode, as well as the transient heat transfer mode [49].

The load characteristics of the ALTEC-11 thermoelectric modules, developed at the Institute of Thermoelectricity of the National Academy of Sciences and the Ministry of Education and Science of Ukraine, which are characterized by increased values of the maximum temperature difference [50].

In the case when the ambient temperature is 25 °C and using a radiator with two 120 x 120 mm^2 fans, one can expect a temperature difference between the radiator and the liquid of 5 ÷ 10 °C at a dissipation power of 200 ÷ 300 W. Thus, one radiator is enough for two thermoelectric modules. The liquid temperature will be 30 – 35 °C.

The temperature losses at the thermal contacts between the thermoelectric modules and the liquid heat exchanger, as well as between the thermoelectric modules and the copper plate when using the KPT-8 thermally conductive paste with a gap h = 0.5 mm will be:

$$\Delta T = \frac{140\,\mathrm{W}\cdot 5\cdot 10^{-5}\,\mathrm{m}}{0.5\,\mathrm{W/mK}(40\cdot 10^{-3})^2\,\mathrm{m}^2} = 8.75^{\circ}\mathrm{C}\,. \qquad (8)$$

However, if we improve the density and bring the gap size to $h = 0.005$ mm, then $\Delta T = 0.9$ °C, that is, about 2 °C for two such heat spreaders.

To these losses, it is also necessary to add the temperature difference between the liquid heat exchanger and the liquid, which will depend on the speed of pumping the liquid.

The dependence of the cold side temperature of thermoelectric modules on the heat flow from the working tool and the fluid pumping speed in the liquid heat exchanger system was calculated, based on the temperature difference of the ALTEC-011 thermoelectric modules for a given heat flow (Fig. 4, 5).

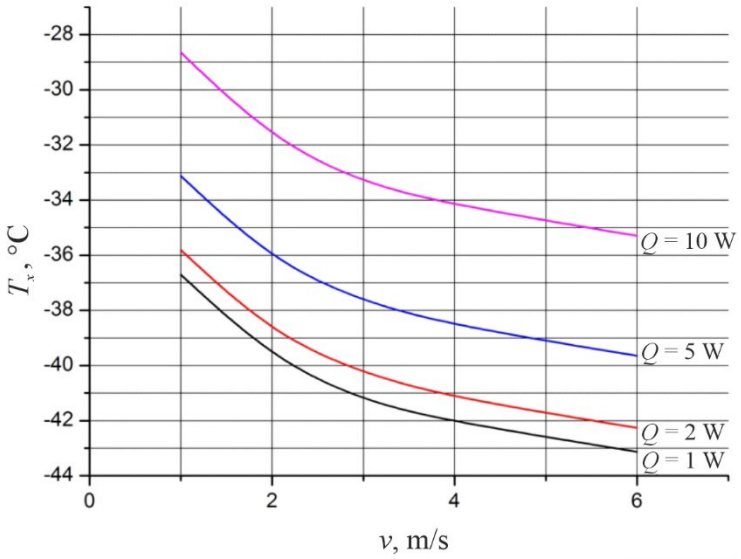

Fig. 4. Dependences of cold side temperature of thermoelectric modules on the heat in-leak from the working tool

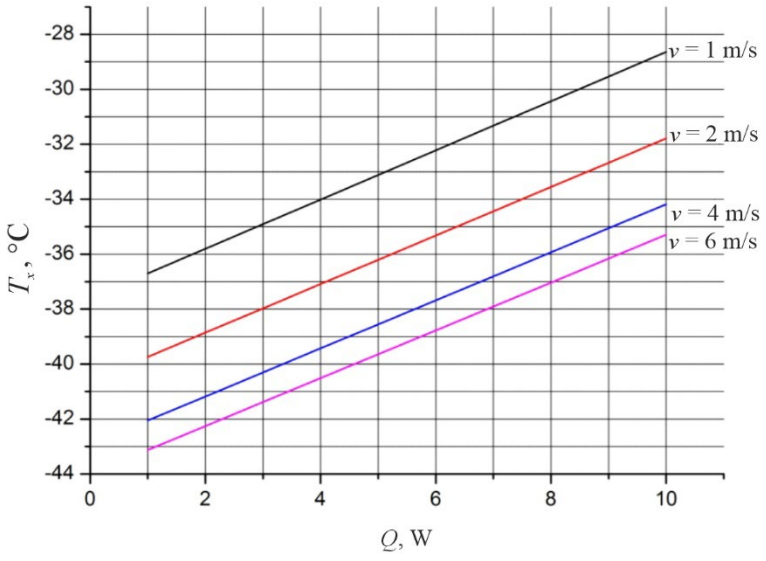

Fig. 5. Dependences of cold side temperature of thermoelectric modules on liquid pumping speed

As studies have shown, the in-leak value is 2 W, which allows for a plate temperature of about – 43 ºC.

2.2. Calculation of the working tool design

The temperature distributions in the working tool and tumor for heating and cooling modes were investigated, which made it possible to optimize the working tool.

Figs. 6 – 7 show typical temperature distributions and isothermal surfaces in the cooling mode.

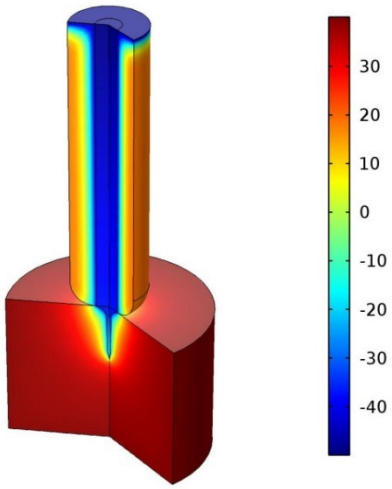

Fig. 6. Temperature distribution in the working tool and tumor in the cooling mode

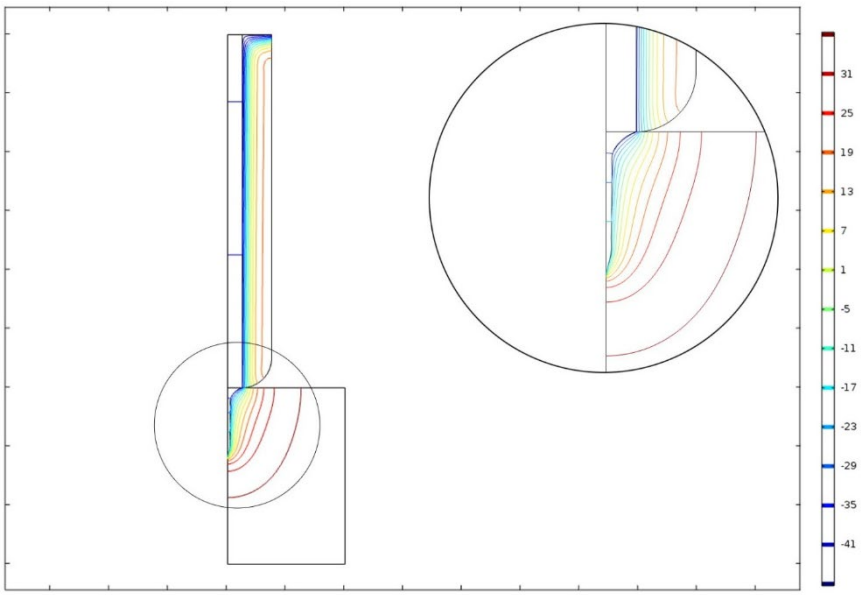

Fig. 7. Isothermal surfaces in the working tool and tumor in the cooling mode

In the cooling mode, the temperature distributions and isothermal surfaces are obtained based on the maximum possible cooling capacity and temperature differences in practice, which makes it possible to obtain the two-stage thermoelectric module ALTEC-011.

The working tool of the device was optimized. The dependences of the freezing depth on the diameter and length of the working tool, the dependences of the freezing depth and needle temperature on the thickness of the working tool insulation, and the dependences of the freezing depth and needle temperature on the needle diameter were determined.

Fig. 8 shows a typical temperature distribution in the working tool and biological tissue in the cooling mode. For this case: rod diameter – 8 mm, rod length – 40 mm, insulation thickness – 5 mm, needle length – 7 mm, needle diameter – 2 mm. Curves 1, 2 – isotherms – 1 and – 8 ºC, respectively. The temperature distribution along the radius of the hemisphere of thermal impact of the working tool of the device – line R, which is shown in Fig. 8, is given in Fig. 9.

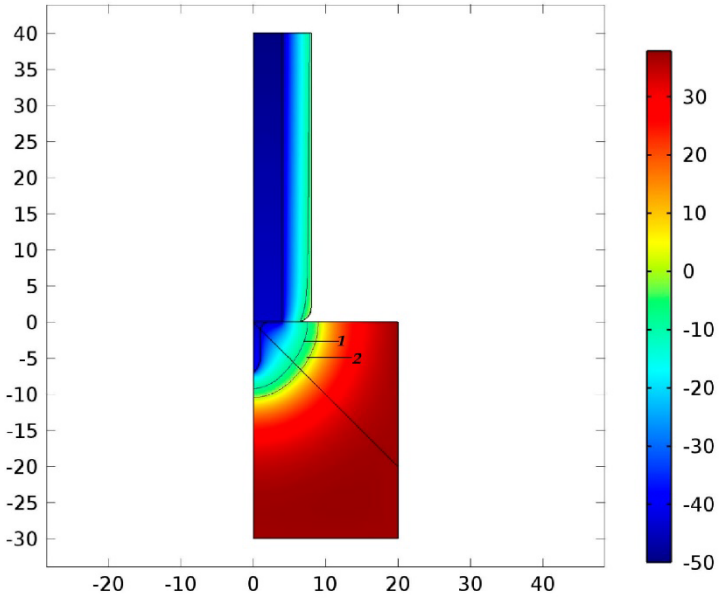

Fig. 8. Typical temperature distribution in the working tool and biological tissue in the cooling mode

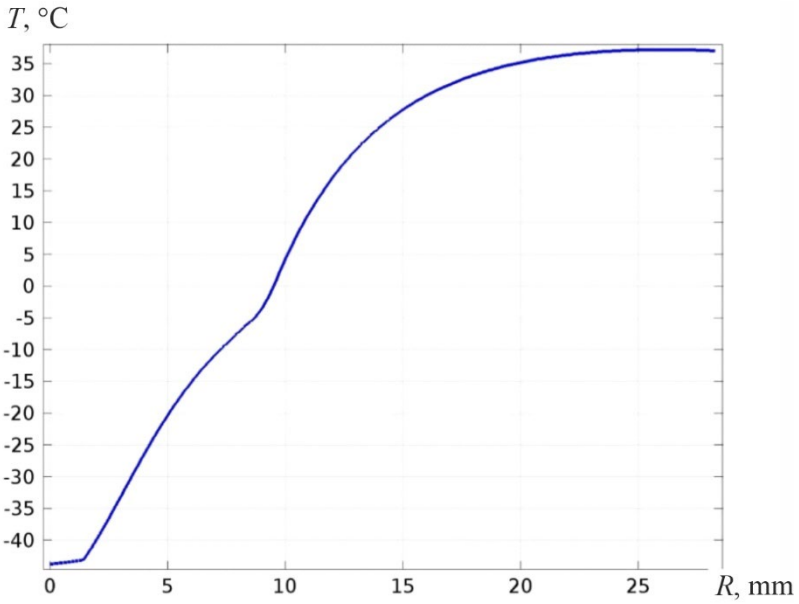

Fig. 9. Temperature distribution along the radius of the hemisphere of thermal impact of the device for the cooling mode

Figs. 10 – 14 show the dependence of the needle temperature and the depth of freezing of biological tissue on the diameter of the rod at different rod lengths. Table 2 shows the values of the needle temperature, freezing depth, temperature at a distance of 5 mm from the center of the needle and heat flow from the rod for different values of the geometric dimensions of the rod. Insulation thickness h_{is} = 5 mm, needle diameter d_n = 2 mm, needle length h_n = 7 mm.

Table 2

Influence of the geometric dimensions of the working tool rod on the freezing depth, needle temperature and heat flow to the cold sides of the modules

Rod length, mm	Rod diameter, mm	Needle temperature, ºC	Temperature at the point R = 5 mm, ºC	Distance to the point with temperature – 8 ºC, mm	Distance to the point with temperature – 1 ºC, mm	Heat flow from the rod, W
10	2	– 35.43	– 10.67	5.71	7.17	1.806
	4	– 45.32	– 15.44	6.79	8.31	2.223
	6	– 47.37	– 19.06	7.51	9,07	2.575
	8	– 48.13	– 22.86	8,28	9.9	3.004
20	2	– 26.5	– 6.6	4.62	6.06	1.472
	4	– 41.38	– 13.63	6.41	7.89	2.111
	6	– 45.19	– 17.96	7.30	8.82	2.535
	8	– 46.67	– 22.01	8.13	9.7	2.999
40	2	– 16.03	4.9	3	4.37	1.098
	4	– 34.79	– 10.62	5.7	7.16	1.93
	6	– 41.16	– 15.9	6.88	8.41	2.467
	8	– 43.84	– 20.4	7.82	9.39	2.989
60	2	– 10.13	14.5	1.83	3.15	0.898
	4	– 29.47	– 8.22	5.06	6.51	1.791
	6	– 37.51	– 14.06	6.5	7.99	2.408
	8	– 41.17	– 18.9	7.55	9.12	2.979
80	2	– 5.94	20.25	–	2.16	0.783
	4	– 25.08	– 6.02	4.47	5.92	1.684
	6	– 34.19	– 12.38	6.13	7.58	2.358
	8	– 38.63	– 17.46	7.28	8.79	2.972

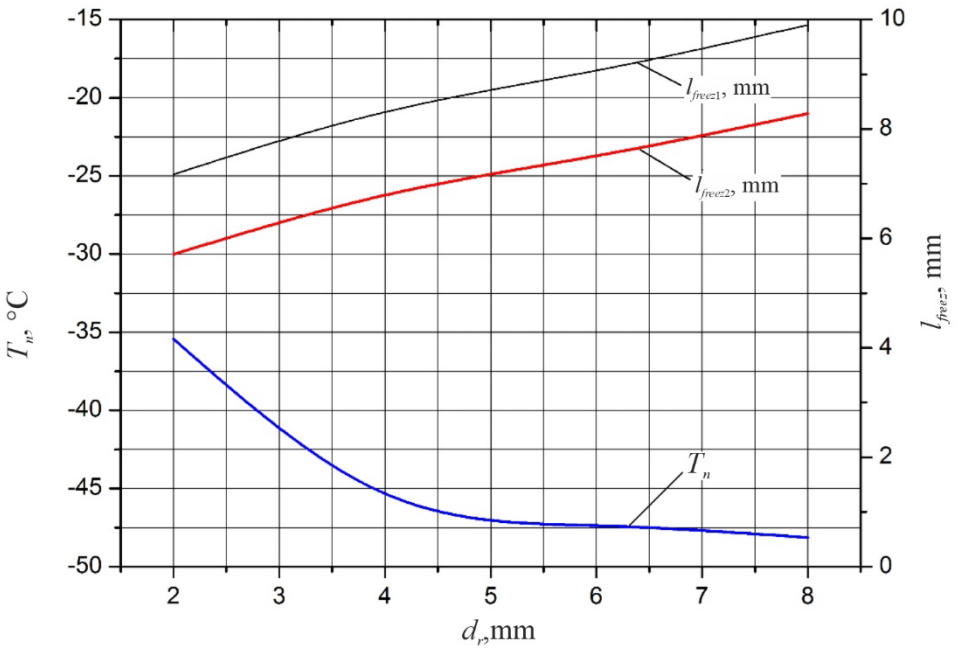

Fig. 10. Dependences of needle temperature (T_n) and freezing depth (l_{freez1} – distance to the isotherm with a temperature of – 1°C, l_{freez2} – distance to the isotherm with a temperature of – 8 °C) on the rod diameter (rod length 10 mm)

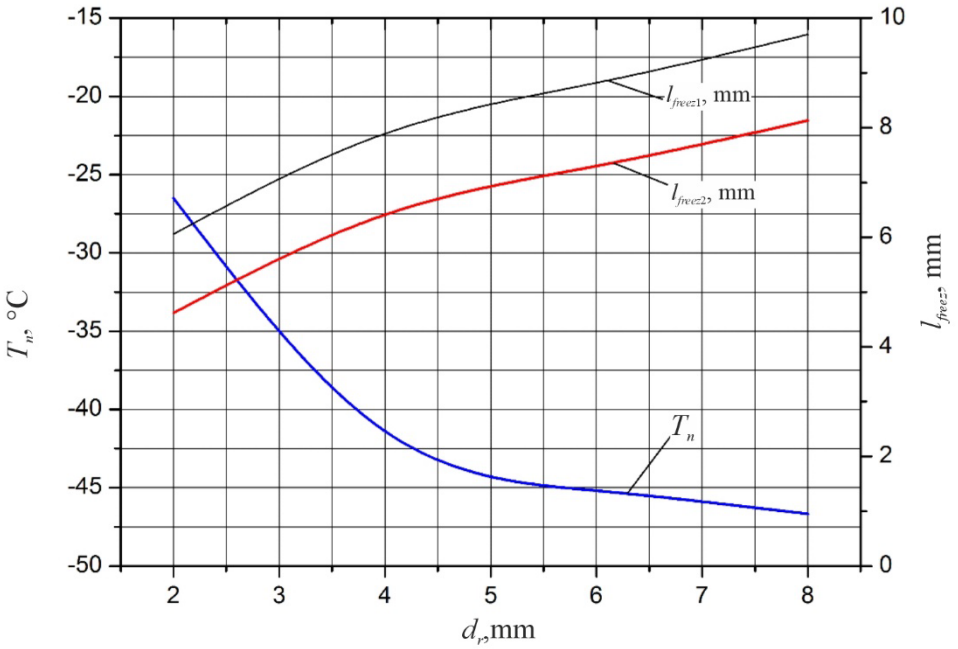

Fig. 11. Dependences of needle temperature (T_n) and freezing depth (l_{freez1} – distance to the isotherm with a temperature of – 1 °C, l_{freez2} – distance to the isotherm with a temperature of – 8 °C) on the rod diameter (rod length 20 mm)

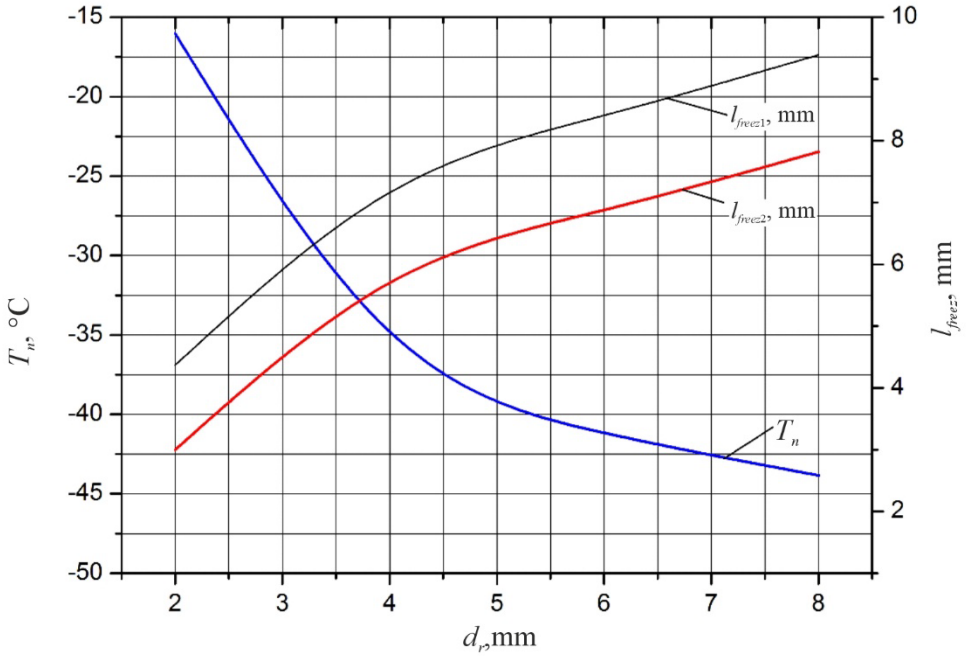

Fig. 12. Dependences of needle temperature (T_n) and freezing depth (l_{freez1} – distance to the isotherm with a temperature of – 1 °C, l_{freez2} – distance to the isotherm with a temperature of – 8 °C) on the rod diameter (rod length 40 mm)

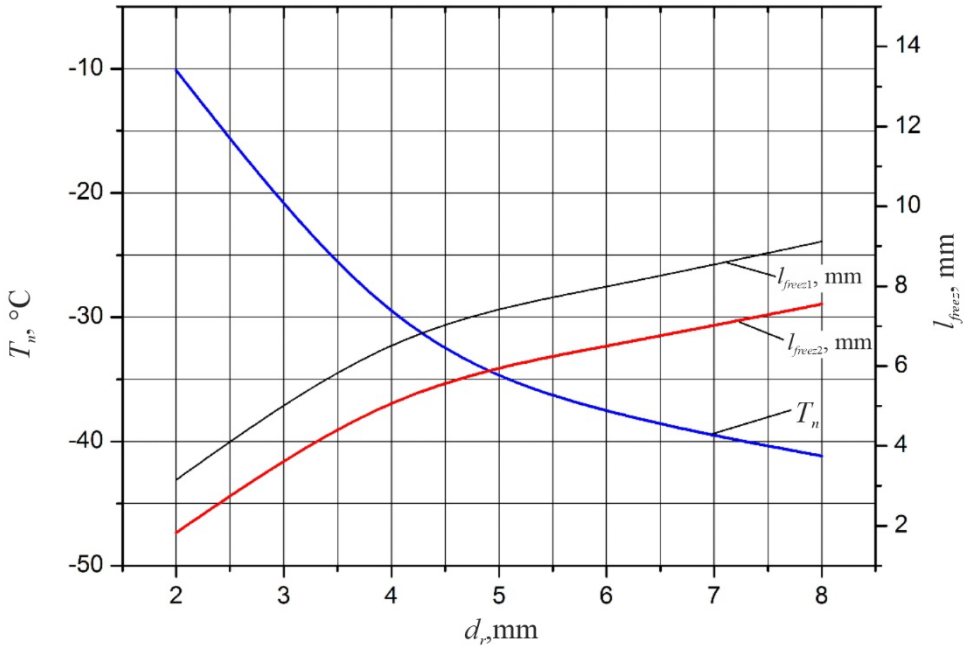

Fig. 13. Dependences of needle temperature (T_n) and freezing depth (l_{freez1} – distance to the isotherm with a temperature of – 1 °C, l_{freez2} – distance to the isotherm with a temperature of – 8 °C) on the rod diameter (rod length 60 mm)

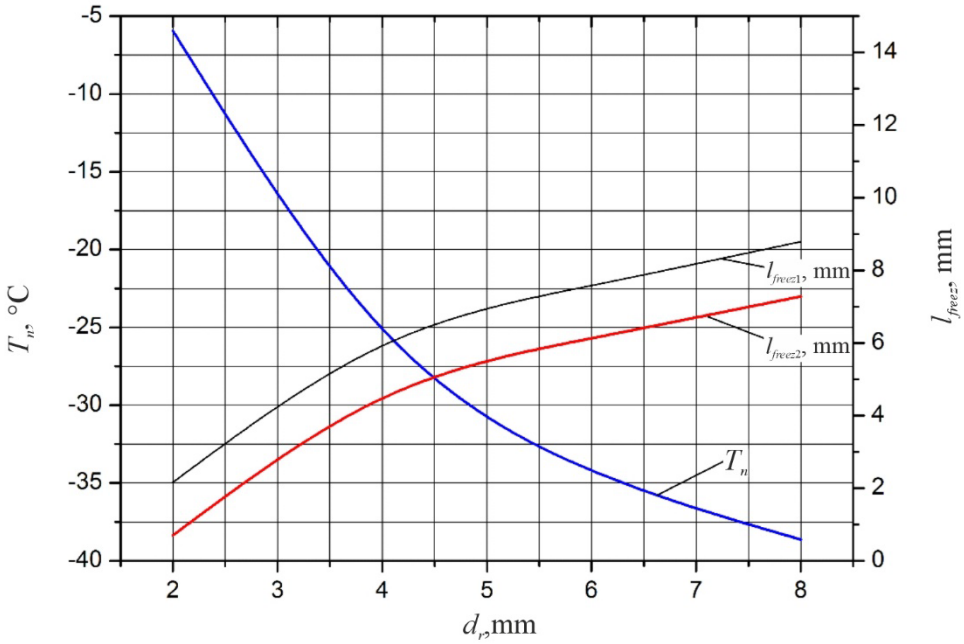

Fig. 14. Dependences of needle temperature (T_n) and freezing depth (l_{freez1} – distance to the isotherm with a temperature of – 1 °C, l_{freez2} – distance to the isotherm with a temperature of – 8 °C) on the rod diameter (rod length 80 mm)

Table 3 shows the values of the needle temperature, freezing depth, temperature at a distance of 5 mm from the center of the needle, and heat flow from the rod for different values of insulation thickness.

Table 3

Impact of insulation thickness on freezing depth, needle temperature, and heat flow to the cold sides of thermoelectric modules

Insulation thickness, Mm	Needle temperature, ºC	Temperature at the point R = 5 mm, ºC	Distance to the point with temperature – 8 ºC, mm	Distance to the point with temperature – 1 ºC, mm	Heat flow from the rod, W
2	– 43.76	– 20.24	7.78	9.35	3.057
3	– 43.79	– 20.29	7.79	9.37	3.027
4	– 43.82	– 20.34	7.81	9.38	3.005
5	– 43.84	– 20.4	7.82	9.39	2.989

Dependences of the needle temperature and freezing depth on the insulation thickness are shown in Fig. 15. The rod diameter d_r = 8 mm, the rod length l_r = 40 mm, the needle diameter d_n = 2 mm, the needle length h_n = 7 mm.

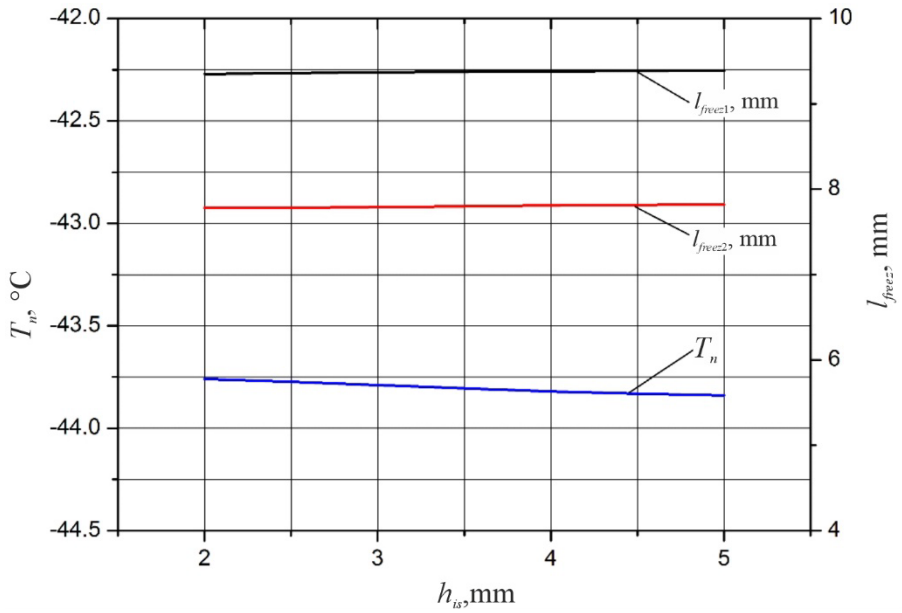

Fig. 15. Dependences of needle temperature (T_n) and freezing depth (h) on the insulation thickness (d_e = 1 mm, h_e = 10 mm, h_{cm} = 80 mm)

Table 4 shows the values of the needle temperature, freezing depth, temperature at a distance of 5 mm from the center of the needle and heat flow from the rod for different values of the needle diameter. The dependences of the needle temperature and freezing depth on the needle diameter are shown in Fig. 16. Rod diameter d_r = 8 mm, rod length l_r = 40 mm, insulation thickness h_{is} = 5 mm, needle length h_n = 7 mm.

Table 4

Impact of needle diameter on freezing depth, needle temperature, and heat flow to the cold sides of thermoelectric modules

Needle diameter, Mm	Needle temperature °C	Temperature at the point R = 5 mm, °C	Distance to the point with temperature – 8 °C, mm	Distance to the point with temperature – 1 °C, mm	Heat flow from the rod, W
05	– 44.71	– 14.8	6.61	8.1	2.517
1	– 44.31	– 17.02	7.12	8.62	2.718
2	– 43.84	– 20.4	7.82	9.39	2.989
3	– 43.35	– 23.5	8.43	10.02	3.267

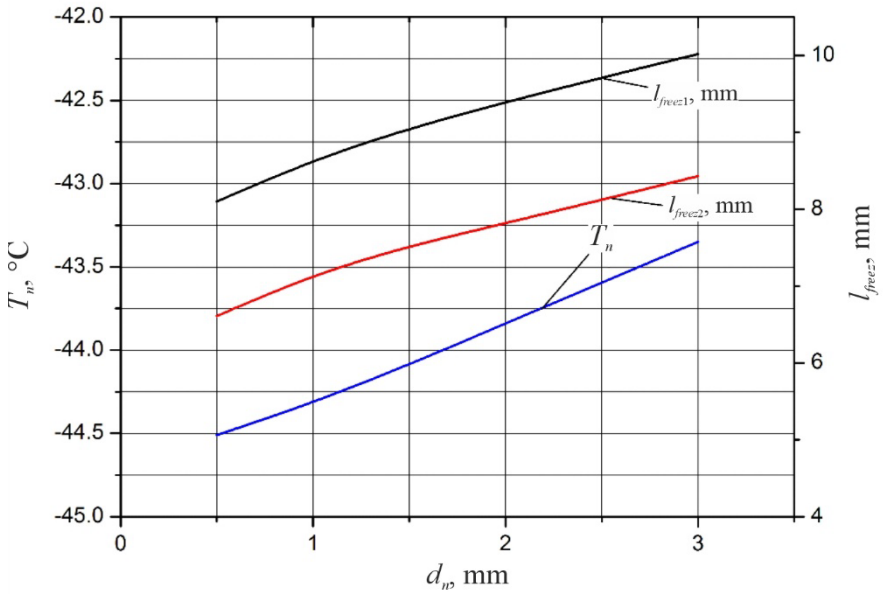

Fig. 16. Dependences of the needle temperature (T_n) and freezing depth (h) on the needle diameter (d_r = 8 mm, l_r = 40 mm, h_{is} = 5 mm, h_n = 7 mm)

Table 5 shows the values of the needle temperature, freezing depth, temperature at a distance of 5 mm from the center of the needle and heat flow from the rod for different values of the needle length. The dependences of the needle temperature and freezing depth on the needle length are shown in Fig. 17. The rod diameter d_r = 8 mm, the rod length l_r = 40 mm, the insulation thickness h_{is} = 5 mm, the needle diameter d_n = 2 mm.

Table 5

Impact of needle length on the freezing depth, needle temperature and heat flow to the cold sides of thermoelectric modules

Needle length, Mm	Needle temperature, °C	Temperature at the point R = 5 mm, °C	Distance to the point with temperature – 8 °C, mm	Distance to the point with temperature – 1 °C, mm	Heat flow from the rod, W
5	– 44.48	– 18.37	7.25	8.69	2.735
7	– 43.84	– 20.4	7.82	9.39	2.989
10	– 43.35	– 23.5	8.35	10.04	3.349
15	– 41.81	– 20.56	8.6	10.59	3.843

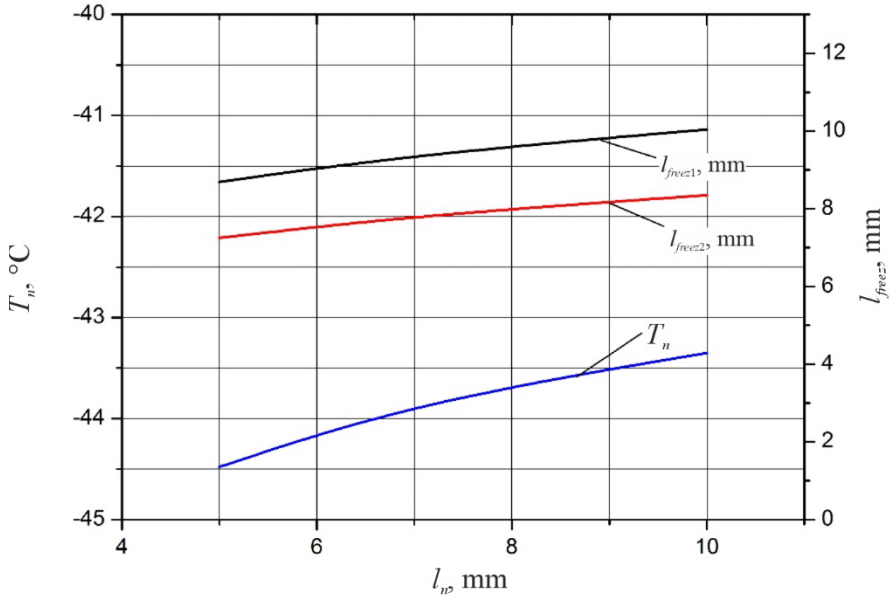

Fig. 17. Dependences of needle temperature (T_n) and freezing depth (h) on the needle length (d_r = 8 mm, l_r = 40 mm, $h_{із}$ = 5 мм, d_n = 2 mm)

The obtained results allow selecting the design of a thermoelectric device and a working tool for a specific treatment method, and also form the basis for the development and manufacture of a thermoelectric device for cryodestruction of biological tissues, in particular oncological neoplasms.

Conclusions

1. A physical, mathematical and computer model of a thermoelectric device for cryodestruction has been created, allowing one to predict the results of local temperature impact on biological tissue during cryodestruction of oncological neoplasms for a specific design of the working tool, based on the necessary treatment conditions.
2. The temperature distributions in biological tissue with an oncological neoplasm and a working tool in the cooling mode were determined.
3. Computer optimization of the working tool and calculation of the heat removal system of thermoelectric modules for the thermoelectric cryodestruction device were carried out.
4. A method for computer calculation of the temperature impact on biological tissues has been developed, which allows obtaining temperature distributions inside biological tissue and predicting the depth of freezing during cryodestruction.

Authors' information

R.R. Kobylianskyi – Cand. Sc. (Phys.-Math.).
O.I. Ivaschuk – M.D., Professor.
V.Yu. Bodiaka – M.D., Professor.
R.V. Fedoriv – Postgraduate.

References

1. Anatychuk, L. I. (1998). *Thermoelectricity: Vol. 1. Physics of Thermoelectricity*. Kyiv-Chernivtsi: Institute of Thermoelectricity.
2. Anatychuk, L. I. (2003). *Thermoelectricity: Vol. 2. Thermoelectric power converters*. Kyiv-Chernivtsi: Institute of Thermoelectricity.
3. Anatychuk, L. I., & Vikhor, L. N. (2012). *Thermoelectricity: Vol. IV. Functionally graded thermoelectric materials*. Kyiv-Chernivtsi: Institute of Thermoelectricity.
4. Vikhor, L., & Kotsur, M. (2023). Evaluation of efficiency for miniscale thermoelectric converter under the influence of electrical and thermal resistance of contacts. *Energies, 16*(10), 4082. https://doi.org/10.3390/en16104082
5. Anatychuk, L. I., & Lysko, V. V. (2020). *Thermoelectricity: Vol. 5. Metrology of thermoelectric materials*. Chernivtsi: Bukrek.
6. Anatychuk, L. I., & Lysko, V. V. (2012). Modified Harman's method. *AIP Conference Proceedings, 1449*, 373–376. https://doi.org/10.1063/1.4731495
7. Anatychuk, L. I., Havryliuk, M. V., & Lysko, V. V. (2015). Absolute method for measuring thermoelectric properties of materials. *Materials Today: Proceedings, 2*(2), 737–743. https://doi.org/10.1016/j.matpr.2015.07.299
8. Lysko, V. V., Razinkov, V. V., & Havryliuk, M. V. (2024). Equipment for determining the thermal conductivity of thermoelectric materials and the thermal resistance of contact structures using the absolute method. *Journal of Thermoelectricity, 3*, 53–63.
9. Nekhlopochin, O. S., Pilipenko, M. M., & Dubrov, S. O. (2023). Damage to major blood vessels during lumbar dissectomy: Risk factors, diagnostics, methods of surgical correction, features of anesthetic support and intensive care. *Ukrainian Neurosurgical Journal, 29*(3), 3–18.
10. Dobson, G. P. (2020). Trauma of major surgery: A global problem that is not going away. *International Journal of Surgery, 81*, 47–54. https://doi.org/10.1016/j.ijsu.2020.07.032
11. Kushneryk, L. Ya., Seniutovych, R. V., & Ivanskyi, A. E. (2003). Thermoelectric device for surgery of oncodiseases. *Journal of Thermoelectricity, 2*, 81–86.
12. Moskalyk, I. A., & Manyk, O. M. (2013). On the use of thermoelectric cooling in cryodestruction practice. *Journal of Thermoelectricity, 6*, 84–92.
13. Moskalyk, I. A. (2015). On the use of thermoelectric devices in cryosurgery. *Physics and Chemistry of the Solid State, 4*, 742–746.
14. Miller, P., & Metzner, D. (1969). Cryosurgery for tumors of the head and neck. *Transactions of the American Ophthalmological and Otolaryngological Society, 73*(2), 300–309.
15. D'Hont, G. (1974). La cryotherapie en ORL. *Acta Otorhinolaryngologica Belgica, 28*(2), 274–278.
16. Mazur, P. (1968). Physical-chemical factors underlying cell injury in cryosurgical freezing. In R. W. Rand, A. P. Rinfret, & H. Leden (Eds.), *Cryosurgery* (pp. 32–51). Springfield, IL: Charles C Thomas Publisher.
17. Hu, B., Shi, X.-L., Zou, J., & Chen, Z.-G. (2022). Thermoelectrics for medical applications: Progress, challenges, and perspectives. *Chemical Engineering Journal, 437*(Part 2), 135359. https://doi.org/10.1016/j.cej.2022.135359

18. Yang, S., Li, Y., Deng, L., Tian, S., Yao, Y., Yang, F., Feng, C., Dai, J., Wang, P., & Gao, M. (2023). Flexible thermoelectric generator and energy management electronics powered by body heat. *Microsystems & Nanoengineering, 9*, 106. https://doi.org/10.1038/s41378-023-00532-4
19. Bause, H. (2004). Kryotherapie lokalisierter klassischer, neues Verfahren mit Peltier-Elementen (–32 °C): Erfahrungsbericht Hamangiome. *Monatsschrift für Kinderheilkunde, 152*, 16–22.
20. Anatychuk, L. I., Ivaschuk, O. I., Kobylianskyi, R. R., Postevka, I. D., Bodiaka, V. Yu., & Gushul, I. Ya. (2016). Thermoelectric device for temperature and heat flux density measurement "ALTEC-10008". *Journal of Thermoelectricity, 1*, 74–81.
21. Anatychuk, L. I., Kobylianskyi, R. R., Konstantinovich, I. A., Lys'ko, V. V., Puhantseva, O. V., Rozver, Y. Yu., & Tiumentsev, V. A. (2016). Calibration bench for thermoelectric converters of heat flux. *Journal of Thermoelectricity, 5*, 65–72.
22. Anatychuk, L. I., Vikhor, L. M., Kobylianskyi, R. R., Kadeniuk, T. Y., & Zvarych, O. V. (2017). Computer simulation and optimization of the dynamic operating modes of thermoelectric reflexotherapy device. *Journal of Thermoelectricity, 3*, 65–74.
23. Anatychuk, L. I., Vikhor, L. M., Kobylianskyi, R. R., & Kadeniuk, T. Y. (2017). Computer simulation and optimization of the dynamic operating modes of thermoelectric device for treatment of skin diseases. *Journal of Thermoelectricity, 2*, 46–59.
24. Anatychuk, L. I., Pasechnikova, N. V., Naumenko, V. O., Zadorozhnyi, O. S., Danyliuk, S. L., Havryliuk, M. V., Tiumentsev, V. A., & Kobylianskyi, R. R. (2020). Thermoelectric device for contact cooling of the human eye. *Physics and Chemistry of Solid State, 21*(1), 140–145.
25. Anatychuk, L. I., Kobylianskyi, R. R., & Kadenyuk, T. Y. (2017). Computer simulation of local thermal effect on human skin. *Journal of Thermoelectricity, 1*, 62–70.
26. Anatychuk, L. I., Pasyechnikova, N. V., Naumenko, V. A., Kobylianskyi, R. R., & Gavrilyuk, N. V. (2019). A thermoelectric device for ophthalmic heat flux density measurements: Results of piloting in healthy individuals. *Oftalmologicheskii Zhurnal*, *(3)*, 45–51.
27. Havryliuk, M. V., & Konstantynovych, I. A. (2014). Thermoelectric device for electrophoresis. *Naukovy visnyk Chernivetskoho Universytetu. Fizyka. Elektronika – Scientific Bulletin of Chernivtsi University. Physics. Electronics*, *3*(1), 101–104.
28. Kobylianskyi, R. R., Kobylianska, A. K., & Fedoriv, R. V. (2024). Computer simulation of temperature distributions in the human heart during cryoablation. *Journal of Thermoelectricity*, *(3)*, 23–35.
29. Kobylianskyi, R. R., Lysko, V. V., & Boychuk, V. V. (2024). Computer-aided design of thermoelectric microcalorimetric sensors. *Journal of Thermoelectricity*, *(1–2)*, 97–112.
30. Kobylianskyi, R. R., Zadorozhnyi, O. S., Umanets, M. M., Pasyechnikova, N. V., Rozver, Y. Yu., & Babich, A. O. (2024). Computer simulation of a thermoelectric device for controlling the temperature of irrigation fluid during ophthalmological operations. *Journal of Thermoelectricity*, *(1–2)*, 61–71.

31. Kobylianskyi, R., Przystupa, K., Lysko, V., Majewski, J., Vikhor, L., Boichuk, V., Zadorozhnyy, O., Kochan, O., Umanets, M., & Pasyechnikova, N. (2025). Thermoelectric measuring equipment for perioperative monitoring of temperature and heat flux density of the human eye in vitreoretinal surgery. *Sensors, 25*(4), Article 999. https://doi.org/10.3390/s25040999
32. Anatychuk, L. I., Kobylianskyi, R. R., & Fedoriv, R. V. (2022). Computer simulation of the working tool of a thermoelectric device for cryodestruction with account of the phase transition. *Journal of Thermoelectricity*, *(3–4)*, 18–30.
33. Gill, W., & Fraser, I. (1968). A look at cryosurgery. *Scottish Medical Journal*, *13*, 268–273.
34. Van Venrjy, G. (1975). Freeze-etching: Freezing velocity and crystal size at different size locations in samples. *Cryobiology*, *12*(1), 46–61.
35. COMSOL AB. (2018). *COMSOL Multiphysics User's Guide* (710 p.).
36. Pennes, H. H. (1948). Analysis of tissue and arterial blood temperatures in the resting forearm. *Journal of Applied Physiology*, *1*(2), 93–122.
37. Lim, H. L., & Gunasekaran, V. (2011). *Mathematical modeling of heat distribution during cryosurgery*. https://isn.ucsd.edu/courses/beng221/problems/2011/project10.pdf
38. Myers, R. S., Hammond, W. G., & Ketcham, A. S. (1970). Cryosurgical necrosis of the head of the pancreas. *Annals of Surgery*, *171*(3), 413–418.
39. Deng, Z. S., & Liu, J. (2005). Numerical simulation of selective freezing of target biological tissues following injection of solutions with specific thermal properties. *Cryobiology*, *50*, 183–192.
40. Jiang, S. C., Ma, N., Li, H. J., & Zhang, X. X. (2002). Effects of thermal properties and geometrical dimensions on skin burn injuries. *Burns*, *28*, 713–717.
41. Cetingul, M. P., & Herman, C. (2008). Identification of skin lesions from the transient thermal response using infrared imaging technique. *IEEE*, 1219–1222.
42. Ciesielski, M., Mochnacki, B., & Szopa, R. (2011). Numerical modeling of biological tissue heating. Admissible thermal dose. *Scientific Research of the Institute of Mathematics and Computer Science*, *1*(10), 11–20.
43. Filipoiu, F., Bogdan, A. I., & Carstea, I. M. (2010). Computer-aided analysis of the heat transfers in skin tissue. In *Proceedings of the 3rd WSEAS Int. Conference on Finite Differences - Finite Elements - Finite Volumes - Boundary Elements* (pp. 53–59).
44. Carstea, D., Carstea, I., & Carstea, I. M. (2011). Interdisciplinarity in computer-aided analysis of thermal therapies. *WSEAS Transactions on Systems and Control*, *6*(4), 115–124.
45. Shah, V. N., Orlov, O. I., Orlov, C., Takebe, M., Thomas, M., & Plestis, K. (2018). Combined cryo-maze procedure and mitral valve repair through a ministernotomy. *Multimedia Manual of Cardiothoracic Surgery*. https://doi.org/10.1510/mmcts.2018.022
46. Rykaczewski, K. (2019). Modeling thermal contact resistance at the finger-object interface. *Temperature*, *6*(1), 85–95.
47. Beliayev, M. M. (1989). *Fundamentals of heat transfer*. Kyiv: Vyscha shkola.
48. ITE. http://ite.cv.ua/

Submitted: 27.02.2025

Кобилянський Р.Р.[1,2] (https://orcid.org/0000-0002-4664-3162),
Іващук О.І.[3] (https://orcid.org/0000-0003-1747-2648),
Бодяка В.Ю.[3] (https://orcid.org/0000-0003-1422-6652),
Федорів Р.В[1] (https://orcid.org/0009-0005-4487-9365)

[1]Чернівецький національний університет імені Юрія Федьковича,
вул. Коцюбинського 2, Чернівці, 58012, Україна
[2]Інститут термоелектрики НАН та МОН України,
вул. Науки, 1, Чернівці, 58029, Україна;
[3]Буковинський державний медичний університет,
Театральна площа, 2, Чернівці, 58002, Україна

Комп'ютерна оптимізація робочого інструменту термоелектричного приладу для кріодеструкції

У роботі наведено результати комп'ютерного моделювання температурного впливу на біологічну тканину з онкологічним новоутворенням у режимі охолодження. Побудовано фізичну, математичну і комп'ютерну моделі біологічної тканини з онкологічним новоутворенням із врахуванням теплофізичних процесів, кровообігу, теплообміну, процесів метаболізму та фазового переходу. Проведено комп'ютерну оптимізацію робочого інструменту та розрахунок системи тепловідводу термоелектричних модулів для термоелектричного приладу кріодеструкції. Визначено розподіли температури у біологічній тканині та охолоджуючому робочому інструменті. Отримані результати дають можливість визначати глибину промерзання біологічної тканини, зокрема онкологічного новоутворення, при заданому температурному впливі. Розроблено методику комп'ютерного розрахунку температурного впливу на біологічні тканини, що дозволяє отримувати розподіли температур всередині біологічної тканини та прогнозувати глибину промерзання при проведенні кріодеструкції.

Ключові слова: термоелектрика, термоелектричний прилад, робочий інструмент, комп'ютерна оптимізація, комп'ютерне моделювання, кріодеструкція, температурний вплив, режим охолодження, розподіл температури, біологічна тканина, онкологічне новоутворення.

Надійшла до редакції: 27.02.2025